Consequences of Oxidation in Nonplanar Porphyrins: Molecular Structure and Diamagnetism of the π Cation Radical of Copper(II) Octaethyltetraphenylporphyrin

Mark W. Renner,[1a] Kathleen M. Barkigia,[1a] Yun Zhang,[1a] Craig J. Medforth,[1b] Kevin M. Smith,[1b] and Jack Fajer*,[1a]

Contribution from the Department of Applied Science, Brookhaven National Laboratory, Upton, New York 11973, and Department of Chemistry, University of California, Davis, California 95616

Received May 23, 1994®

Abstract: Crystal structures are reported for the sterically crowded porphyrin Copper(II) 2,3,7,8,12,13,17,18-octaethyl-5,10,15,20-tetraphenylporphyrin (Cu(OETPP), **1**) and its π cation radical Cu(OETPP)$^{\bullet+}ClO_4^-$ (**2**). **1** was chosen to assess the consequences of oxidation in a nonplanar porphyrin on the expectation that its multiple peripheral substituents not only induce an S4 saddle conformation on the macrocycle but should also prevent the dimerizations in the solid that have complicated several previous crystallographic studies of porphyrin π cation radicals. Interest in the consequences of oxidation arises from the presence of nonplanar bacteriochlorophylls in photosynthetic reaction centers in which the chromophores lie in van der Waals contact so that even small structural changes induced by electron transfer would alter the electronic coupling between the π cation and anion radicals generated by the primary photochemical charge separation. Oxidation of **1** does indeed result in further conformational changes in **2**: an additional ruffling is imposed on the original saddle shape of **1** in which the pyrrole rings twist, the *meso* carbons move alternately up and down out of the porphyrin plane by ~0.2 Å, and the phenyl groups rotate further into that plane by more than 10°. The additional distortions are attributed to changes in electronic configuration due to the oxidation *and* to the low-energy barriers between nonplanar conformers with different degrees of nonplanarity predicted by previous molecular mechanics calculations. OETPPs retain their saddle conformations in solution because of the steric crowding of the multiple substituents. **2** thus provides a test of the proposal by Reed, Scheidt, and co-workers (e.g., *J. Am. Chem. Soc.* **1987**, *109*, 2644) that the conformations of porphyrin π cation radicals comprised of paramagnetic metals control magnetic coupling with the metals and that nonplanar macrocycles exhibit antiferromagnetic coupling. **2** displays optical and FT-IR spectral signatures diagnostic of a π cation radical in solution, but it is EPR-silent, and its NMR spectrum clearly indicates a diamagnetic species. The Cu(II) and the nonplanar π radical spins in **2** are thus indeed antiferromagnetically coupled, in accord with the above proposal. The saddle conformation of **1** destabilizes the π system of the macrocycle and causes the molecule to be readily oxidized with molecular iodine, a mild oxidizing agent. Unexpectedly, the radical crystallized in the presence of excess I_2 carries a discrete I_7^- counterion. We report here the first example and structure of such a large polyiodide anion to be stabilized by a porphyrin cation: Cu(OETPP)$^{\bullet+}I_7^-$ (**3**). Crystallographic data. $CuN_4C_{60}H_{60}$ (**1**): triclinic space group $P\bar{1}$, a = 13.888(4) Å, b = 16.820(3) Å, c = 13.222(3) Å, α = 97.33(2)°, β = 107.97(2)°, γ = 103.52(2)°, V = 2843.3 Å^3, Z = 2, R_F = 0.057 and R_{wF} = 0.086 based on 7391 reflections with $F_o > 3\sigma F_o$, T = 298 K. $CuN_4C_{60}H_{60}{}^{\bullet+}ClO_4^-\cdot CH_2Cl_2$ (**2**): monoclinic space group $P2_1/n$, a = 11.896(1) Å, b = 24.242(5) Å, c = 19.090(3) Å, β = 100.73(1)°, V = 5408.8 Å^3, Z = 4, R_F = 0.048 and R_{wF} = 0.049 based on 4570 reflections with $F_o > 3\sigma F_o$, T = 298 K. $CuN_4C_{60}H_{60}{}^{\bullet+}I_7^-$ (**3**): monoclinic space group $P2_1$, a = 13.108(17) Å, b = 18.332(14) Å, c = 13.683(10) Å, β = 107.88(8)°, V = 3129.2 Å^3, Z = 2, R_F = 0.101 and R_{wF} = 0.117 based on 2269 reflections with $F_o > 4\sigma F_o$, T = 200 K.

Introduction

Recent crystallographic determinations of antenna and reaction center bacteriochlorophyll (BChl) protein complexes have established that the chromophores adopt multiple nonplanar conformations.[2-4] The axial ligands, hydrogen bonds, and neighboring residues that comprise the microenvironments of the photosynthetic chromophores may thus define a protein scaffolding that controls the conformations of the molecules.[5] Theoretical calculations indicate that such structural variations shift the frontier orbitals of BChls and thereby can modulate their optical, redox and electron transfer properties.[6]

An expanding body of structural data for isolated porphyrins and hydroporphyrins further illustrates the considerable flexibility of such molecules and the significant distortions that can be imposed on porphinoid macrocycles by crystal packing and steric effects.[7,8] Several recent crystallographic studies have led to the concept of "conformationally designed" porphyrins whereby the introduction of multiple peripheral substituents induces large deformations of the macrocycles that minimize steric interactions between the substituents.[6,9-12] In particular, crystal structure determinations of the Cu(II), Co(II), Zn(II), Ni(II), diacid salt, and free base derivatives of 2,3,7,8,12,13,17,18-octaethyl-5,10,-

* Abstract published in *Advance ACS Abstracts*, September 1, 1994.

(1) (a) Brookhaven National Laboratory. (b) University of California, Davis.

(2) Tronrud, D. E.; Schmid, M. F.; Matthews, B. W. *J. Mol. Biol.* **1986**, *188*, 443.

(3) Deisenhofer, J.; Michel, H. *Science* **1989**, *245*, 1463 and references therein.

(4) Yeates, T. O.; Komiya, H.; Chirino, A.; Rees, D. C.; Allen, J. P.; Feher, G. *Proc. Natl. Acad. Sci. U.S.A.* **1988**, *85*, 7993. El-Kabbani, O.; Chang, C. H.; Tiede, D.; Norris, J. R.; Schiffer, M. *Biochemistry* **1991**, *30*, 5361.

(5) Huber, R. *Eur. J. Biochem.* **1990**, *187*, 283.

(6) (a) Barkigia, K. M.; Chantranupong, L.; Smith, K. M.; Fajer, J. *J. Am. Chem. Soc.* **1988**, *110*, 7566. b) Gudowska-Nowak, E.; Newton, M. D.; Fajer, J. *J. Phys. Chem.* **1990**, *94*, 5795.

(7) Scheidt, W. R.; Lee, J. H. *Struct. Bonding (Berlin)* **1987**, *64*, 1.

(8) Barkigia, K. M.; Fajer, J. In *The Photosynthetic Reaction Center*; Deisenhofer, J., Norris, J. R., Eds.; Academic Press: San Diego, CA, 1993; Vol. II, p 513.

0002-7863/94/1516-8582$04.50/0

15,20-tetraphenylporphyrin (OETPP)[9] have established that the molecules all adopt severely saddled conformations in which the pyrrole rings move alternately up and down with displacements of the pyrrole β carbons from the mean porphyrin core greater than 1 Å and that the phenyl rings rotate into the planes of the macrocycles with average dihedral angles of ~45°. NMR, resonance Raman, and EXAFS results clearly indicate that the nonplanar configurations of the OETPPs are maintained in solution.[9] Furthermore, molecular mechanics calculations and variable-temperature NMR results suggest large energy barriers (10–20 kcal/mol) to flattening the molecules.[9,13] The significantly altered optical, redox, EPR, NMR, vibrational, and excited singlet and triplet properties of OETPPs in solution[9,13–16] thus reflect the nonplanarity of the molecules and begin to offer some insights into the effects conformational variations may have on the properties of photosynthetic chromophores (or porphyrinic prosthetic groups) in proteins.

We extend here our studies on conformational effects to consider the structural consequences of oxidizing a nonplanar porphyrin. The question is particularly relevant to electron transfer in photosynthetic reaction centers since the primary BChl donors and acceptors[17a] lie in van der Waals contact *in vivo*[3,4] and even small conformational changes would alter the distances between the molecules and the electronic coupling between them.[17b] Further, although the photoinduced redox reactions yield π cation and anion radicals with extensively delocalized charges,[17] the changes in spin distribution in the macrocycles and of the charges on the magnesiums of the BChls may be expected to alter the interactions of the chromophores with their immediate environment, particularly with axial ligands, hydrogen bonds, and polarizable neighboring residues,[18] and thus change the protein pocket in which the molecules sit. Conformational substates of the excited or ground state chromophore–protein complexes or of the chromophores themselves have already been evoked in order to rationalize the inhomogeneous kinetics of primary charge separation in reaction centers.[6,19] As well, EPR and ENDOR studies of the oxidized BChls in single crystals of reaction centers suggest at least some reorientation of peripheral groups compared to the structures in the unoxidized ground state.[20]

Several crystallographic studies of isolated porphyrin π cation radicals have sought to assess the structural consequences of oxidation.[7,21–23] Not surprisingly, for extensively delocalized π radicals, oxidations cause only small changes in the porphyrin bond distances, on the order of ~0.05 Å or less. (Recall, however, that the difference between carbon–carbon single and double bonds is only ~0.2 Å). Significant conformational modifications often do accompany oxidations.[7,21–23] However, the results are complicated by aggregation of the radicals, particularly in the case of tetra- and pentacoordinated *meso* tetraaryl derivatives where the resulting saddle deformations of the π radicals are attributed to dimerization in the crystals.[7,23]

In a different context, an interesting outcome of the structural studies of π cation radicals was the observation by Scheidt, Reed, and co-workers that the conformations of cation radicals incorporating paramagnetic metals influence the magnetic coupling between the metal and radical.[22,23] These authors proposed that, in planar macrocycles, the metal d orbitals and the radical π orbitals (a_{2u} or a_{1u}[24]) are orthogonal and result in ferromagnetic coupling whereas, in nonplanar radicals, overlap of the orbitals is allowed and results in antiferromagnetic coupling. The clearest examples are found with Cu(II) radicals.[23] $Cu^{II}(TPP)^{\bullet+}$[25] crystallizes as saddle-shaped dimers which are diamagnetic whereas, in solution, the species is paramagnetic[26] and presumed to be planar.[23] In agreement with the latter assumption, crystalline $Cu^{II}(TMP)^{\bullet+}$ which is planar is paramagnetic with $S = 1$.[23]

We report here spectroscopic and structural results for Cu^{II}(OETPP) and its π cation radical. Besides imposing a significant saddling[27] on the macrocycle,[9b] the multiple peripheral substituents should also prevent aggregation of the molecules. Indeed, both the neutral compound and its radical are monomeric in the crystalline state. Oxidation induces additional deformations of the porphyrin skeleton; the radical $Cu(OETPP)^{\bullet+}ClO_4^-$ is more distorted than the parent compound and exhibits some ruffling

(9) (a) Barkigia, K. M.; Berber, M. D.; Fajer, J.; Medforth, C. J.; Renner, M. W.; Smith, K. M. *J. Am. Chem. Soc.* **1990**, *112*, 8851. (b) Sparks, L. D.; Medforth, C.J.; Park, M. S.; Chamberlain, J. R.; Ondrias, M. R.; Senge, M. O.; Smith, K. M.; Shelnutt, J. A. *J. Am. Chem. Soc.* **1993**, *115*, 581. (c) Barkigia, K. M.; Renner, M. W.; Furenlid, L. R.; Medforth, C. J.; Smith, K. M.; Fajer, J. *J. Am. Chem. Soc.* **1993**, *115*, 3627. (d) Regev, A.; Galili, T.; Medforth, C. J.; Smith, K. M.; Barkigia, K. M.; Fajer, J.; Levanon, H. J. Phys. Chem. **1994**, *98*, 2520. (e) Barkigia, K. M.; Fajer, J.; Berber, M. D.; Smith, K. M. *Acta Crystallogr.*, in press.

(10) Mandon, D.; Ochsenbein, P.; Fischer, J.; Weiss, R.; Jayaraj, K.; Austin, R. N.; Gold, A.; White, P. S.; Brigaud, O.; Battioni, P.; Mansuy, D. *Inorg. Chem.* **1992**, *31*, 2044. Ochsenbein, P.; Ayougou, K.; Mandon, D.; Fischer, J.; Weiss, R.; Austin, R. N.; Jayaraj, K.; Gold, A.; Terner, J.; Fajer, J. *Angew. Chem., Int. Ed. Engl.* **1994**, *33*, 348.

(11) Renner, M. W.; Cheng, R. J.; Chang, C. K.; Fajer, J. *J. Phys. Chem.* **1990**, *94*, 8508. Cheng, R. J.; Chen, Y. R.; Wang, S. L.; Cheng, C. Y. *Polyhedron* **1993**, *12*, 1353. Bhyrappa, P.; Krishnan, V.; Nethaji, M. *J. Chem. Soc., Dalton Trans.* **1993**, 1901.

(12) Henling, L. M.; Schaefer, W. P.; Hodge, J. A.; Hughes, M. E.; Gray, H. B. *Acta Crystallogr.* **1993**, *C49*, 1743.

(13) Shelnutt, J. A.; Medforth, C. J.; Berber, M. D.; Barkigia, K. M.; Smith, K. M. *J. Am. Chem. Soc.* **1991**, *113*, 4077. Medforth, C. J.; Senge, M. O.; Smith, K. M.; Sparks, L. D.; Shelnutt, J. A. *J. Am. Chem. Soc.* **1992**, *114*, 9859.

(14) Forman, A.; Renner, M. W.; Fujita, E.; Barkigia, K. M.; Evans, M. W.; Smith, K. M.; Fajer, J. *Isr. J. Chem.* **1989**, *29*, 57.

(15) Gentemann, S.; Medforth, C. J.; Forsyth, T. P.; Nurco, D. J.; Smith, K. M.; Fajer, J.; Holten, D. *J. Am. Chem. Soc.* **1994**, *116*, 7363.

(16) Stichternath, A.; Schweitzer-Stenner, R.; Dreybrodt, W.; Mak, R. S. W.; Li, X.; Sparks, L. D.; Shelnutt, J. A.; Medforth, C. J.; Smith, K. M. *J. Phys. Chem.* **1993**, *97*, 3701. Piffat, C.; Melamed, D.; Spiro, T. G. *J. Phys. Chem.* **1993**, *97*, 7441.

(17) (a) Arlt, T.; Schmidt, S.; Kaiser, W.; Lauterwasser, C.; Meyer, M.; Scheer, H.; Zinth, W. *Proc. Natl. Acad. Sci. U.S.A.* **1993**, *90*, 11757. (b) For a review, see: Bixon, M.; Fajer, J.; Feher, G.; Freed, J. H.; Gamliel, D.; Hoff, A. J.; Levanon, H.; Mobius, K.; Nechustai, R.; Norris, J. R.; Scherz, A.; Sessler, J. L.; Stehlik, D. *Isr. J. Chem.* **1992**, *32*, 369.

(18) See, e.g.: Shreve, A. P.; Cherepy, N. J.; Franzen, S.; Boxer, S. G.; Mathies, R.A. *Proc. Natl. Acad. Sci. U.S.A.* **1991**, *88*, 11207. Nabedryk, E.; Robles, S. J.; Goldman, E.; Youvan, D. C.; Breton, J. *Biochemistry* **1992**, *31*, 10852. Maiti, S.; Cowen, B. R.; Diller, R.; Iannone, M.; Moser, C. C.; Dutton, P. L.; Hochstrasser, R. M. *Proc. Natl. Acad. Sci. U.S.A.* **1993**, *90*, 5247. Palaniappan, V.; Martin, P. C.; Chynwat, V.; Frank, H. A.; Bocian, D. F. *J. Am. Chem. Soc.* **1993**, *115*, 12035 and references therein.

(19) Kirmaier, C.; Holten, D. *Proc. Natl. Acad. Sci. U.S.A.* **1990**, *87*, 3552. Vos, M. H.; Rappaport, F.; Lambry, J. C.; Breton, J.; Martin, J. L. *Nature* **1993**, *363*, 320. Gehlen, J. N.; Marchi, M.; Chandler, D. *Science* **1994**, *263*, 499. Gudowska-Nowak, E. *J. Phys. Chem.* **1994**, *98*, 5257. Wang, Z.; Pearlstein, R. M.; Jia, Y.; Fleming, G. R.; Norris, J. R. *Chem. Phys.* **1993**, *176*, 421.

(20) Lendzian, F.; Huber, M.; Isaacson, R. A.; Endeward, B.; Plato, M.; Bonigk, B.; Mobius, K.; Lubitz, W.; Feher, G. *Biochim. Biophys. Acta* **1993**, *1183*, 139.

(21) Spaulding, L. D.; Eller, P. G.; Bertrand, J. A.; Felton, R. H. *J. Am. Chem. Soc.* **1974**, *96*, 982. Barkigia, K. M.; Spaulding, L. D.; Fajer, J. *Inorg. Chem.* **1983**, *22*, 349. Song, H.; Orosz, R. D.; Reed, C. A.; Scheidt, W. R. *Inorg. Chem.* **1990**, *29*, 4274. Scheidt, W. R.; Cheng, B.; Haller, K. J.; Mislankar, A.; Rae, A. D.; Reddy, K. V.; Song, H.; Orosz, R. D.; Reed, C. A.; Cukiernik, F.; Marchon, J. C. *J. Am. Chem. Soc.* **1993**, *115*, 1181. Kim, H. J.; Whang, D.; Kim, J.; Kim, K. *Inorg. Chem.* **1992**, *31*, 3882.

(22) Buisson, G.; Deronzier, A.; Duee, E.; Gans, P.; Marchon, J. C.; Regnard, J. R. *J. Am. Chem. Soc.* **1982**, *104*, 6793. Gans, P.; Buisson, G.; Duee, E.; Marchon, J. C.; Erler, B. S.; Scholz, W. F.; Reed, C. A. *J. Am. Chem. Soc.* **1986**, *108*, 1223.

(23) Scholz, W. F.; Reed, C. A.; Lee, Y. J.; Scheidt, W. R.; Lang, G. *J. Am. Chem. Soc.* **1982**, *104*, 6791. Erler, B. S.; Scholz, W. F.; Lee, Y. J.; Scheidt, W. R.; Reed, C. A. *J. Am. Chem. Soc.* **1987**, *109*, 2644. Song, H.; Reed, C. A.; Scheidt, W. R. *J. Am. Chem. Soc.* **1989**, *111*, 6865.

(24) Fajer, J.; Davis, M. S. *The Porphyrins*; Dolphin, D., Ed.; Academic Press: New York, 1979; Vol. IV, p 197.

(25) Abbreviations used in the text: TPP = 5,10,15,20-tetraphenylporphyrin, OEP = 2,3,7,8,12,13,17,18-octaethylporphyrin, TMP = 5,10,15,20-tetramesitylporphyrin, Br_8(TPFP) = 2,3,7,8,12,13,17,18-octabromo-5,10,15,20-tetrakis(pentafluorophenyl)porphyrin.

(26) Godziela, G. M.; Goff, H. M. *J. Am. Chem. Soc.* **1986**, *108*, 2237.

(27) The nomenclature is that suggested by Scheidt and Lee.[7] In a saddle conformation, the pyrrole rings are alternately tilted above and below the average plane through the 24 atoms of the porphyrin core and the *meso* atoms lie approximately in that plane. In a ruffled conformation, alternate pyrrole rings are twisted clockwise or anticlockwise about the metal–nitrogen bond and the *meso* carbon atoms sit alternately above or below the average porphyrin plane.

Table 1. Experimental Crystallographic Details

formula	$CuN_4C_{60}H_{60}$	$CuN_4C_{60}H_{60}{}^{\bullet+}ClO_4^-\cdot CH_2Cl_2$	$CuN_4C_{60}H_{60}{}^{\bullet+}I_7^-$
crystallized from	CH_2Cl_2/hexane	CH_2Cl_2/hexane	CD_2Cl_2
fw	900.71	1085.1	1789.0
space group	$P\bar{1}$	$P2_1/n$	$P2_1$
Z	2	4	2
T (K)	298	298	200
a (Å)	13.888(4)	11.896(1)	13.108(17)
b (Å)	16.820(3)	24.242(5)	18.332(14)
c (Å)	13.222(3)	19.090(3)	13.683(10)
α (deg)	97.33(2)	90.0	90.0
β (deg)	107.97(2)	100.73(1)	107.88(8)
γ (deg)	103.52(2)	90.0	90.0
V (Å^3)	2843.3	5408.8	3129.2
crystal color	irregular red	irregular black	irregular black
crystal shape	parallepiped	prism	parallepiped
density calcd (g/cm^3)	1.072	1.332	1.899
dimensions (mm)	0.42 × 0.10 × 0.12	0.55 × 0.40 × 0.20	0.32 × 0.17 × 0.15
μ (cm^{-1})	8.023	23.47	282.2
λ (Å)	1.5418	1.5418	1.5418
instrument	CAD-4	CAD-4	CAD-4
no. of reflns measd	11619	6075	3541
no. of reflns unique	9728	5725	3169
no. of reflns used	7391 ($F_o > 3\sigma(F_o)$)	4570 ($F_o > 3\sigma(F_o)$)	2269 ($F_o > 4\sigma(F_o)$)
2θ range (deg)	4–140	4–100	4–100
data measd	$h\pm k\pm l$	$hk\pm l$	$hk\pm l$
corrections to the data	Lp	Lp	Lp and decay
absorption correction	empirical (based on ψ scans)	empirical (based on ψ scans)	empirical Fourier method
structure solution/refinement	Multan78, Shelxs-86/MolEN	Multan80/MolEN	SIR, DIRDIF/MolEN
R_F	0.057	0.048	0.101
R_{wF}	0.086	0.049	0.117

superimposed on the saddle conformation.[27] In accord with the postulates of Scheidt, Reed, et al.,[23] the nonplanar radical is *diamagnetic* in solution, as evidenced by its NMR spectrum.

We have previously noted that the saddle distortions of the OETPP series destabilize the π systems of the molecules and render the compounds easier to oxidize than the corresponding OEP or TPP derivatives.[6,9a,c] The trend holds for Cu(OETPP) as well, and the compound is readily oxidized with molecular iodine, a mild oxidizing agent. Unexpectedly, however, the radical generated and crystallized in the presence of excess I_2 carries a discrete I_7^- counterion. Although polyiodide anions are not uncommon and are usually associated with large cations,[28,29] Cu(OETPP)$^{\bullet+}I_7^-$ represents the first example of a porphyrin cation stabilizing a discrete heptaiodide anion.[30]

Method

The synthesis of Cu(OETPP) has been reported.[9b] Cu(OETPP)-d_{20} (deuterated phenyl groups) was prepared in the same manner with benzaldehyde-d_5. For spectroscopic studies, Cu(OETPP)$^{\bullet+}ClO_4^-$ was generated by addition of a slight excess of anhydrous $AgClO_4$ to a solution of the porphyrin in dry CH_2Cl_2, followed by filtration to remove the metallic Ag. The reaction was monitored optically (see below). The formation of Cu(OETPP)$^{\bullet+}I^-$ was similarly monitored during addition of I_2. Crystals of Cu(OETPP)$^{\bullet+}ClO_4^-$ suitable for X-ray diffraction were obtained by slow diffusion of *n*-hexane into a concentrated CH_2Cl_2 solution of the radical. Crystals of Cu(OETPP)$^{\bullet+}I_7^-$ were obtained by slow evaporation of an NMR sample of Cu(OETPP) in CD_2Cl_2 to which a large excess of I_2 had been added to ensure complete oxidation of the paramagnetic parent compound.

Redox potentials were determined by cyclic voltammetry at a Pt electrode (vs SCE) with 0.1 M Bu_4NClO_4 as the supporting electrolyte on a BAS 100A electrochemical analyzer. Optical spectra of the oxidized species were also obtained by controlled potential electrolysis in an OTTLE cell equipped with CaF_2 windows[31] that allowed spectra to be recorded throughout the ultraviolet, visible, and infrared regions (Bu_4NPF_6 was used as the electrolyte for IR measurements). Solvents and electrolyte salts were purified by standard techniques.[31] Optical spectra were obtained on Cary 2300 or Hewlett Packard 8452A diode array spectrophotometers. FT-IR spectra in the OTTLE cell or in KBr pellets were recorded on a Mattson Polaris spectrometer. EPR spectra at X-band were acquired on a Bruker-IBM ER 200D instrument. ^1H and ^2H NMR spectra were accumulated at 300 and 46 MHz, respectively, on a Bruker AM 300 spectrometer at Brookhaven. The ^1H results were duplicated on a General Electric QE300 instrument at UCD. (Chemical shifts are referenced against tetramethylsilane.)

Crystallography. Details of the data collection and refinements for Cu(OETPP), Cu(OETPP)$^{\bullet+}ClO_4^-$, and Cu(OETPP)$^{\bullet+}I_7^-$ are presented in Table 1. Crystals of all three compounds were mounted on glass fibers. The ClO_4^- and I_7^- species were encapsulated in a rapid-drying epoxy. Data for the latter were obtained at 200 K with an Enraf-Nonius FR558-S cooling system.

Lattice parameters were determined using 25 reflections measured at $\pm 2\theta$ for all samples. Three standard reflections were checked hourly to monitor possible crystal movement and decay. On the basis of analysis of these reflections, an anisotropic decay correction was applied to the I_7^- data.

The structure of a neutral Cu(OETPP) incorporating two molecules of CH_2Cl_2 in the lattice has been reported previously.[9b] Nonetheless, in the present case, the compound was treated as an unknown and its structure was solved with a combination of Multan-80,[32] Shelxs-86,[33] MolEN,[34] and a series of difference Fourier maps.

For the I_7^- salt, a SIR[35] solution indicated eight strong peaks that were assigned to seven iodides and Cu. This heavy atom fragment was expanded

(28) Greenwood, N. N.; Earnshaw, A. *Chemistry of the Elements*; Pergamon Press: Oxford, U.K., 1984; p 978. Wells, A. F. *Structural Inorganic Chemistry*, 5th ed.; Clarendon Press: Oxford, U.K., 1993; p 394.

(29) Poli, R.; Gordon, J. C.; Khanna, R. K.; Fanwick, P. E. *Inorg. Chem.* **1992**, *31*, 3165.

(30) There are several examples of partially oxidized porphyrins and phthalocyanines with I_3^- counterions: Schramm, C. J.; Scaringe, R. P.; Stojakovic, D. R.; Hoffman, B. M.; Ibers, J. A.; Marks, T. J. *J. Am. Chem. Soc.* **1980**, *102*, 6702. Pace, L. J.; Martinsen, J.; Ulman, A.; Hoffman, B. M.; Ibers, J. A. *J. Am. Chem. Soc.* **1983**, *105*, 2612 and references therein.

(31) Zhang, Y.; Gosser, D. K.; Rieger, P. H.; Sweigart, D. A. *J. Am. Chem. Soc.* **1991**, *113*, 4062.

(32) Main, P.; Fiske, S. J.; Hull, S. E.; Lessinger, L.; Germain, G.; Declercq, J. P.; Woolfson, M. M. Multan 80, *A System of Computer Programs for the Automatic Solution of Crystal Structures from X-ray Diffraction Data*, University of York: York, England, 1980.

(33) Sheldrick, G. M. *Crystallographic Computing 3*; Sheldrick, G. M., Kruger, C., Goddard, R., Eds.; Oxford University Press: Oxford, U.K., 1985; p 175.

(34) *MolEN, An Interactive Structure Solution Procedure*; Enraf-Nonius: Delft, The Netherlands, 1990.

(35) Burla, M. C.; Camalli, M.; Cascarano, G.; Giacovazzo, C.; Polidori, G., Spagna, R.; Viterbo, D. *J. App. Crystallogr.* **1989**, *22*, 389.

with DIRDIF,[36] and the model was completed from difference Fourier maps. (The absolute configuration of the compound was checked, and the enantiomer which gave the lower *R* factor was retained.)

All three structures were refined by full-matrix least-squares. For the neutral and ClO_4^- compounds, all non-hydrogen atoms were allowed anisotropic expression of their thermal motion, whereas only the seven iodines and the Cu atom were refined anisotropically in the I_7^- salt until convergence was reached. Hydrogens were included in idealized positions (C–H = 0.95 Å) with their isotropic thermal parameters fixed at 1.2 times those of the atoms to which they are attached. Scattering factors were taken from standard compilations,[37] and anomalous terms for all atoms were included in the refinements. Positional and thermal parameters for all three compounds are included in the supplementary material.

Results and Discussion

Spectroscopic Results. Previous electrochemical results have established that Zn and Ni OEP derivatives are easier to oxidize than their TPP counterparts.[38] In turn, Zn(OETPP)[6,9a] and Ni-(OETPP),[9c] which are hybrids of the two types of porphyrins, are still easier to oxidize. The effect is predicted theoretically and is attributable to the destabilization of the porphyrin π systems caused by the saddle conformations of the molecules.[6,9a,c] Cu-(OETPP) follows the same trend. Cyclic voltammetry of the compound shows two reversible one-electron oxidations in several nonaqueous solvents: $E^1_{1/2}$ and $E^2_{1/2}$ = 0.38 and 0.97 V in CH_2Cl_2, 0.55 and 1.01 V in butyronitrile, and 0.59 and 1.06 V in tetrahydrofuran (THF) vs SCE. The first oxidation potentials are significantly lower than those reported for CuOEP: 0.84 V in CH_2Cl_2[26] and 0.79 V in butyronitrile[39] (and obviously still less than those for Cu(TPP).[38]) Note that the differences between the first and second oxidation potentials ($\Delta E = E^2_{1/2} - E^1_{1/2}$) are larger in CH_2Cl_2 (0.59 V) than in butyronitrile (0.46 V) or in THF (0.47 V) and imply different degrees of solvation and/or pairing with the perchlorate counterions in CH_2Cl_2 and the other two solvents. The effect may be due, in part, to the structural pocket created around the metal by the saddle conformation and the ethyl substituents (see Figure 6).

The optical spectra in THF obtained by controlled potential electrolysis in an OTTLE cell are shown in Figure 1. Both the first and second oxidation products evolve with well-defined isosbestic points and are reversible: better than 95% of the starting products are recovered upon electroreduction. The optical spectra of the two oxidation stages are typical of those found for porphyrin π cation radicals and π dications[40,41] and exclude the possibility that either stage involves the oxidation of Cu(II) to Cu(III). Similar optical spectra are obtained by bulk electrolysis in CH_2Cl_2 except that the relative heights of the two Soret peaks of the cation in the 400–450 nm region are inverted. Chemical oxidations with $AgClO_4$ or I_2 also yield the same spectrum for the cation in CH_2Cl_2 (spectra of the cation in CH_2Cl_2 are included as Figure 1S in the supplementary material).

Porphyrin π cation radicals exhibit diagnostic infrared marker bands at ~1280 cm^{-1} for TPPs and ~1550 cm^{-1} for OEPs.[42] Recall that these radicals display different unpaired spin densities that are determined by the HOMO occupancy of the unpaired electron:[24] in TPPs, an electron is abstracted from the a_{2u} orbital

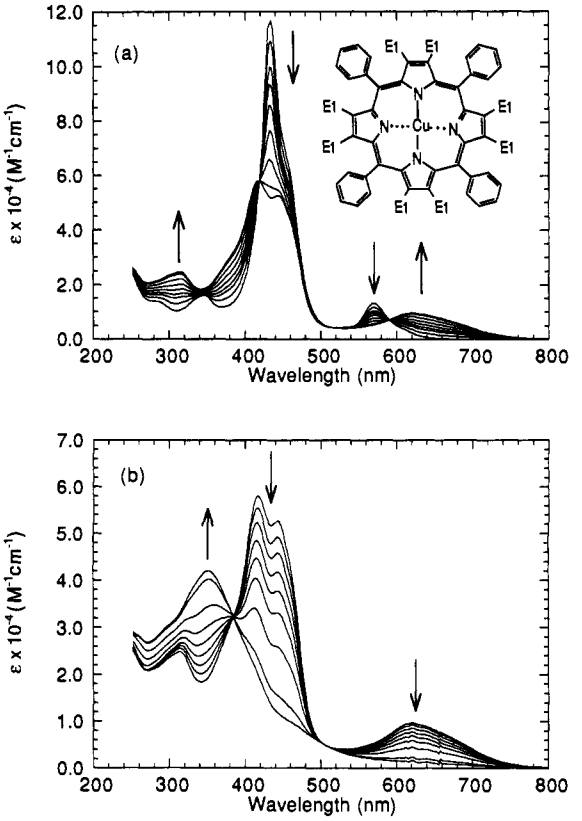

Figure 1. Optical spectra observed upon one- and two-electron electrochemical oxidations of Cu(OETPP) in THF containing 0.1 M Bu_4NClO_4: (a) Cu(OETPP) → Cu(OETPP)$^{\bullet+}$ and (b) Cu(OETPP)$^{\bullet+}$ → Cu(OETPP)$^{2+}$.

(in D_{4h} symmetry) and the resulting unpaired spin density is concentrated at the nitrogens and *meso* carbons, whereas in OEPs, the a_{1u} orbital is left half-occupied with spin density localized principally on the Cα atoms and, to a lesser extent, on the Cβ atoms. Cu(TPP)$^{\bullet+}$ and Cu(OEP)$^{\bullet+}$ have been characterized as a_{2u} and a_{1u} radicals, respectively, on the basis of NMR[26] and resonance Raman results.[43] In KBr pellets, Cu(TPP)$^{\bullet+}ClO_4^-$ [44] and Cu(TPP)$^{\bullet+}SbCl_6^-$ [42] display the diagnostic a_{2u} FT-IR bands at 1289 and 1295 cm^{-1}, respectively, and Cu(OEP)$^{\bullet+}ClO_4^-$, the a_{1u} marker band(s) at 1549 and 1573 cm^{-1}. [44] An additional enhanced band at 1600 cm^{-1} is also observed for the latter in solution.[44] Hu and Spiro[44] have attempted to correlate the two radical spin distributions with the marker bands and, particularly relevant to the ensuing discussion, have assigned the a_{2u} band at 1289 cm^{-1} in Cu(TPP)$^{\bullet+}ClO_4^-$ to ν_{41}, the pyrrole ring stretch which involves the Cα–Cβ and Cα–N bonds.

The FT-IR spectra of Cu(OETPP) (**1**) and of the perchlorate (**2**) and iodide (**3**) Cu(OETPP)$^{\bullet+}$ salts in KBr pellets are compared in Figure 2. The most prominent new band in the oxidized species occurs at 1355 cm^{-1} and corresponds most closely to that at ~1290 cm^{-1} observed in Cu(TPP)$^{\bullet+}$.[42,44] The shift to higher energy may reasonably be attributed to the larger conformational distortions of the macrocycle and, particularly, of the pyrrole rings observed in Cu(OETPP)$^{\bullet+}$ relative to Cu(TPP)$^{\bullet+}$ [23] (see Figure 7). An analogous band appears at 1354 cm^{-1} upon *in situ* electrooxidation of **1** in THF-d_8 solution with Bu_4NPF_6 electrolyte (The concentrations of electrolyte required for bulk electrolysis in the OTTLE cell preclude the use of the Bu_4NClO_4 for IR measurements. The solution FT-IR spectra are included as Figure 2S in the supplementary material.)

Note the absence of new bands in Cu(OETPP)$^{\bullet+}$ that would correspond to the ~1550 cm^{-1} marker band in CuOEP$^{\bullet+}$. (By

(36) Beurskens, P. T. DIRDIF: Application of Direct Methods to Difference Structures for the Solution of Heavy Atom Structures and Expansion of a Molecular Fragment. Lecture Notes, International Summer School on Crystallographic Computing, Meulheim A. D. Ruhr., 1984.
(37) *(37) International Tables for X-ray Crystallography*; Kynoch Press: Birmingham, England, 1974; Vol. IV, p 148.
(38) Felton, R. H. *The Porphyrins*; Dolphin, D., Ed.; Academic Press: New York, 1978; Vol. 5, p 53. Davis, D. G. *Ibid.* p 127.
(39) Fuhrhop, J. H.; Kadish, K. M.; Davis, D. G. *J. Am. Chem. Soc.* **1973**, *95*, 5140.
(40) Wolberg, A.; Manassen, J. *J. Am. Chem. Soc.* **1970**, *92*, 2982.
(41) Fajer, J.; Borg, D. C.; Forman, A.; Dolphin, D.; Felton, R. H. *J. Am. Chem. Soc.* **1970**, *92*, 3451.
(42) Shimomura, E. T.; Phillippi, M. A.; Goff, H. M.; Scholz, W. F.; Reed, C. A. *J. Am. Chem. Soc.* **1981**, *103*, 6778.
(43) Czernuszewicz, R. S.; Macor, K. A.; Li, X. Y.; Kincaid, J. R.; Spiro, T. G. *J. Am. Chem. Soc.* **1989**, *111*, 3861. Oertling, W. A.; Salehi, A.; Chang, C. K.; Babcock, G. T. *J. Phys. Chem.* **1989**, *93*, 1311.
(44) Hu, S.; Spiro, T. G. *J. Am. Chem. Soc.* **1993**, *115*, 12029.

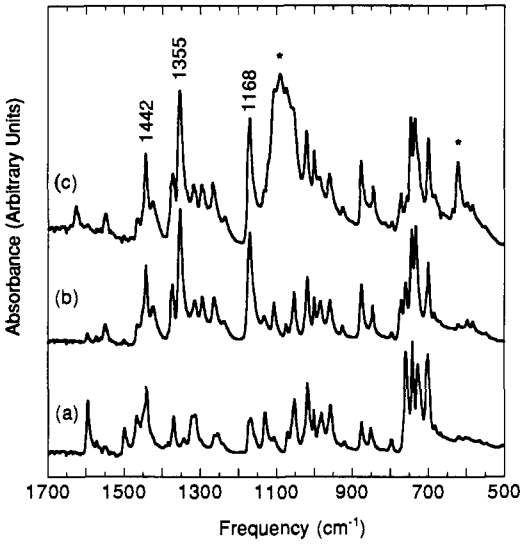

Figure 2. FT-IR spectra in KBr pellets: (a) Cu(OETPP), (b) $Cu(OETPP)^{\bullet+}I^-$, and (c) $Cu(OETPP)^{\bullet+}ClO_4^-$. Bands marked with asterisks in c are due to the ClO_4^- anion.

analogy with assignments made for Ni(OETPP),[16] the bands in Figure 2 centered at ~1440 cm^{-1} are CH_2 scissor modes and those at 1170 cm^{-1} are B_{1g} modes involving Cα–Cβ and Cβ–CH_2.)

The optical spectrum of the oxidized Cu(OETPP) shown in Figure 1a is clearly consonant with a π cation radical. The similarity between the IR marker bands of a_{2u} radicals and that found here for $Cu(OETPP)^{\bullet+}$ suggests that the latter is also an a_{2u} radical. This conclusion is supported by the resolved EPR spectrum of $ZnOETPP^{\bullet+}$, which exhibits[14] the nitrogen hyperfine splittings characteristic of a_{2u} radicals.[24] An additional example of the effect of *meso* phenyl substituents on orbital occupancy is found in the hybrid zinc 5,10,15,20-tetraphenyl tetrabenzoporphyrin: the unsubstituted tetrabenzo π radical is a_{1u}, but introduction of the additional phenyl groups results in an a_{2u} radical.[11]

Cu(II) porphyrins are paramagnetic because of the d^9 configuration of Cu(II). The unpaired electron resides in the $d_{x^2-y^2}$ orbital, which leads to characteristic EPR spectra for Cu(II) porphyrins: four peaks due to the nuclear spin of $^3/_2$ of the Cu and superhyperfine interactions with the four nitrogens of the porphyrin. The spectra in solution are insensitive to the porphyrin peripheral substituents or the nature of the macrocycle itself. Cu(II) porphyrins and hydroporphyrins all display similar features.[45] **1** in CH_2Cl_2 also exhibits a typical Cu(II) porphyrin EPR spectrum as shown in Figure 3. A similation[46] of the experimental spectrum yields $\langle g \rangle = 2.086$, $a_{Cu} = 86.5$ G, and four nitrogens with $a_N = 14.4$ G. The saddle conformation of the complex has little effect on the Cu–N interactions which are slightly smaller than those reported for Cu(TPP), $a_{Cu} = 90.5$ G and $a_N = 15.8$ G, or for CuOEP, $a_{Cu} = 90$ G and $a_N = 15$ G.[45] Upon oxidation to the cation, the EPR signal of **1** in Figure 3 is lost at room temperature or at ~110 K, and there is no evidence of the triplet or aggregate spectra observed in paramagnetic Cu(II) porphyrin π cations at $g = 2$ or at half-field.[26,47] The absence of an EPR signal for $Cu(OETPP)^{\bullet+}$ could result[26] from efficient spin–spin relaxation by noninteracting spins, a large zero-field splitting for an $S = 1$ state, or, as expected for a nonplanar

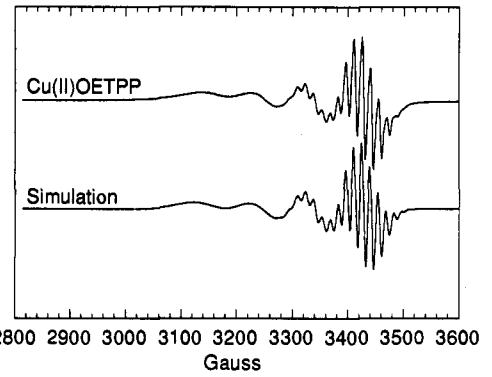

Figure 3. EPR spectrum of Cu(OETPP) in CH_2Cl_2 at 297 K. The simulation assumes $a_{Cu} = 86.5$ G and four nitrogens with $a_N = 14.4$ G.

porphyrin, antiferromagnetic coupling between the Cu(II) and the π radical spins. The following NMR data for $Cu(OETPP)^{\bullet+}$ iodide and perchlorate confirm that the species are indeed diamagnetic in solution.

ENDOR results[48] for Cu(TPP) and NMR data[26] for Cu(TPP) and Cu(OEP) have established that the unpaired electron of Cu(II) interacts with the peripheral substituents of the porphyrins. The ^1H NMR spectrum of **1** is displayed in Figure 4a along with the resonance assignments, which were assigned by their relative areas, line widths, and deuteration of the phenyl groups in Cu(OETPP)-d_{20}. The chemical shifts are listed in Table 2 and compared there to those reported for Cu(OEP) and Cu(TPP) by Godziela and Goff.[26] The phenyl protons of **1** are broadened significantly, and their chemical shifts are comparable to those found for Cu(TPP). However, the methylene groups at the β pyrrole positions are not shifted as much as those in Cu(OEP), presumably because of their significant out-of-plane displacements due to the saddle conformation of **1** (see Figure 7). $Cu(OEP)^{\bullet+}$ and $Cu(TPP)^{\bullet+}$ are paramagnetic in solution ($S = 1$), and deuteration of the radicals, which yields narrowed ^2H NMR lines, was necessary to characterize the radicals.[26] In contrast, **3** (Figure 4b) and **2** exhibit sharp ^1H NMR lines in solution, clearly indicative of *diamagnetic* species. Indeed, the NMR spectra and chemical shifts of $Cu(OETPP)^{\bullet+}$ differ little from those of diamagnetic Zn(OETPP), which also adopts a saddle conformation[9a] (Table 2). (Resonance assignments for **2** and **3** are based on integrated peak areas and decoupling experiments. As in the Zn complex, the ethyl groups exhibit an ABX_3 pattern, assigned to the methyls and two sets of methylene groups, with coupling constants $J_{AB} = 15$ Hz and $J_{AX} = J_{BX} = 7.4$ Hz.) The small differences that are observed for the phenyl and methylene protons in the two compounds likely arise from the more distorted conformation of the Cu radical.

The optical and FT-IR data clearly indicate that the oxidized Cu(OETPP) is a π cation radical. The lack of an EPR signal and the sharp NMR spectrum of the radical are thus best ascribed to strong antiferromagnetic coupling between the Cu(II) and the nonplanar conformation of the macrocycle π radical evident from the NMR data and the crystallographic results that follow.

The antiferromagnetic coupling in $Cu(OETPP)^{\bullet+}$ is thus consonant with the proposal[22,23] that the macrocycle conformations affect the magnetic coupling of porphyrin π cation radicals comprised of paramagnetic metals. A similar conclusion has recently been reached for the Cu(II) π radicals of short chain basket handle porphyrins which are assumed to retain the nonplanar structures of the neutral derivatives upon oxidation.[49]

Crystallographic Results. Figure 5 presents the molecular structures and nomenclatures for neutral **1** and its oxidized perchlorate salt **2**. Before detailing the structural changes that

(45) Murphy, M. J.; Siegel, L. M.; Kamin, H.; Rosenthal, D. *J. Biol. Chem.* **1973**, *248*, 2801. Stolzenberg, A. M.; Spreer, L. O.; Holm, R. H. *J. Am. Chem. Soc.* **1980**, *102*, 364. Richardson, P. F.; Chang, C. K.; Hanson, L. K.; Spaulding, L. D.; Fajer, J. *J. Phys. Chem.* **1979**, *83*, 3420.

(46) Toy, A. D.; Chaston, S. H. H.; Pilbrow, J. R.; Smith, T. D. *Inorg. Chem.* **1971**, *10*, 2219.

(47) Konishi, S.; Hoshino, M.; Imamura, M. *J. Am. Chem. Soc.* **1982**, *104*, 2057. Fujii, H. *Inorg. Chem.* **1993**, *32*, 875.

(48) Brown, T. G.; Hoffman, B. M. *Mol. Phys.* **1980**, *39*, 1073.

(49) Ravikanth, M.; Misra, A.; Chandrashekar, T. K.; Sathaiah, S.; Bist, H. D. *Inorg. Chem.* **1994**, *33*, 392.

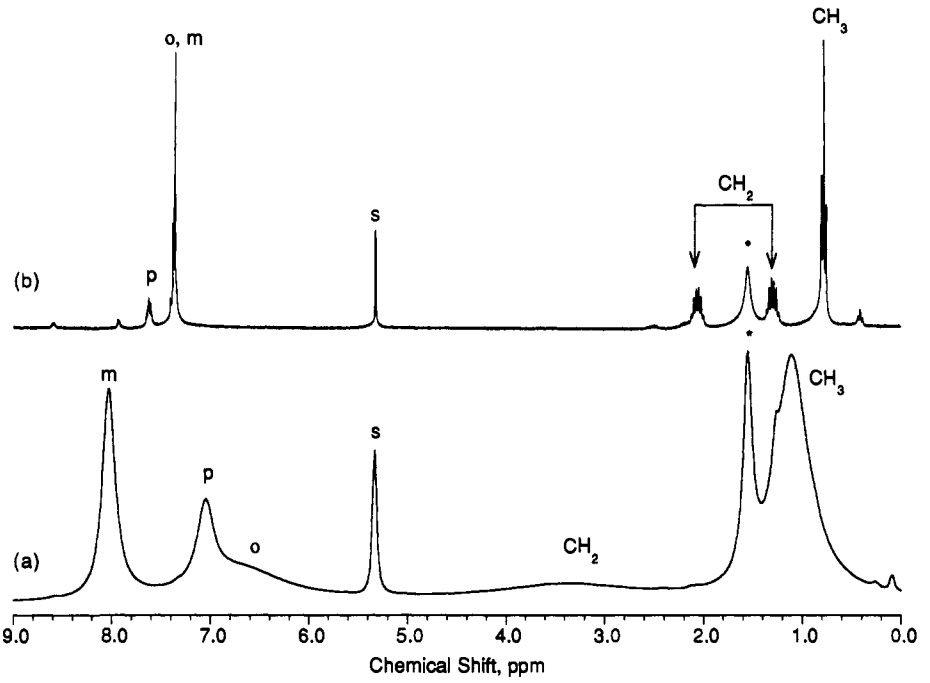

Figure 4. ^1H NMR spectra in CD_2Cl_2 at 297 K: (a) Cu(OETPP) and (b) Cu(OETPP)$^{\bullet+}I^-$ (the same spectrum is obtained for the perchlorate salt). The asterisks mark trace impurities.

Table 2. NMR Chemical Shifts for Cu(II) Porphyrins and Their π Cation Radicals[a]

porphyrin	*o*-phenyl	*m*-phenyl	*p*-phenyl	β-pyrrole	*meso*	$-CH_2-$	$-CH_3$	ref
Cu(TPP)[b]		7.48	7.62	41				26
Cu(TPP)$^{\bullet+}ClO_4^-$	−4.90	15.8	−1.01	13.4				26
Cu(OEP)					−6.2	11.5	1.88	26
Cu(OEP)$^{\bullet+}ClO_4^-$					−4.1	17.1		26
Cu(OETPP)	~6.6[c]	8.03	7.03			~3.3	1.11	
Cu(OETPP)$^{\bullet+}I^-$	7.37	7.37	7.62			2.06, 1.29	0.77	
Cu(OETPP)$^{\bullet+}ClO_4^-$	7.37	7.37	7.64			2.05, 1.30	0.75	
Zn(OETPP)	8.44	7.74	7.74			2.83, 2.24	0.59	9a

[a] In dichloromethane at room temperature, ppm relative to TMS. [b] Data from ref 26 are ^1H and ^2H shifts. [c] ^2H data from Cu(OETPP)-d_{20}.

accompany the oxidation of **1**, we summarize the salient features of the two crystallographic determinations. (Because the seven iodines of Cu(OETPP)$^{\bullet+}I_7^-$ (**3**) dominated the X-ray scattering and the compound decayed slowly during data collection, the precision of the data for the porphyrin in **3** does not warrant detailed comparison with **1** or **2** and the later discussion of **3** will concentrate on the unexpected I_7^- anion.)

Sparks et al.[9b] have recently reported the structure of **1** in space group $P\bar{1}$ at 130 K. The crystal lattice included two CH_2Cl_2 molecules of solvation. The results reported here for **1** at 298 K in the same space group but *without* any solvate molecules agree within 1σ with the low-temperature determination. (The only notable differences in the two structures are the average dihedral angles between the phenyl rings and the mean porphyrin planes: 45.6° at 298 K and 46.8° at 130 K.) These results establish that the saddle conformation[7,27] of **1** (see Figures 6–8) is not temperature dependent nor is it influenced by the presence or absence of molecules of solvation.

In **1**, the Cu lies in the average plane of the four nitrogens, the nitrogens themselves are arranged ~0.15 Å above and below that plane, the *meso* carbons are situated in the average plane, and the geminal β carbons of successive pyrrole rings are displaced alternately above and below the average nitrogen or macrocycle planes by 1.1–1.2 Å. In **2**, the Cu moves ~0.1 Å out-of-plane toward the ClO_4^- counterion, the nitrogens lie in-plane, the *meso* carbons are displaced alternately above and below the average plane by ~0.2 Å, and the pyrrole rings adopt more twisted configurations about the axes that bisect the nitrogens and the Cβ–Cβ bonds. The displacements of the β carbons in **2** range from ~1.2 to 1.5 Å (Figures 7 and 8). The oxidized molecule thus exhibits an additional ruffling deformation[7,27] that is superimposed on the saddle conformation of **1**. In addition, the dihedral angles of the phenyl rings have narrowed significantly: they average 33° in **2** versus 46° in **1**. There are *no* close contacts between adjacent molecules in either structure that would account for the nonplanarity of the compounds (Figure 6).

The two structures are contrasted in greater detail in Figures 6–9 and in the discussion that follows. Their average bond distances and angles are collated and compared to those of saddle-shaped $Cu^{II}Br_8(TPFP)$[12,25] and $Cu^{II}(TPP)^{\bullet+}SbCl_6^-$[23] in Table 3.

The presence of the perchlorate anion clearly indicates that the porphyrin in **2** is a cation. In accord with the spectroscopic evidence presented above that **2** is a π cation radical, the average Cu–N distances of 1.973(4) Å in **1** and 1.974(3) Å in **2** establish that the oxidation of **1** to **2** is centered on the porphyrin rather than the metal: Cu(III)–N distances are typically 0.06–0.08 Å shorter than Cu(II)–N values.[50] As well, the Cu–N distances in **1** and **2** are comparable to those of nonplanar $Cu^{II}Br_8(TPFP)$, 1.971(6) Å,[12] and $Cu^{II}(TPP)^{\bullet+}SbCl_6^-$, 1.988(4) Å.[23] (The slightly longer Cu–N bonds in the latter may result from its shallower saddle distortion relative to that of **2**. Larger deviations from planarity tend to shorten M–N distances.[51])

In **1**, the Cu is centered in the plane of the nitrogens but the nitrogens themselves are arranged "tetrahedrally" about the Cu and deviate by ±0.14 Å from their average plane. In **2**, the

(50) Clark, G. R.; Skelton, B. W.; Waters, T. N. *J. Chem. Soc., Dalton Trans.* **1976**, 1528; *J. Chem. Soc., Chem. Commun.* **1972**, 1163.

(51) Hoard, J. L. In *Porphyrins and Metalloporphyrins*; Smith, K. M., Ed.; Elsevier: Amsterdam, 1975; p 317.

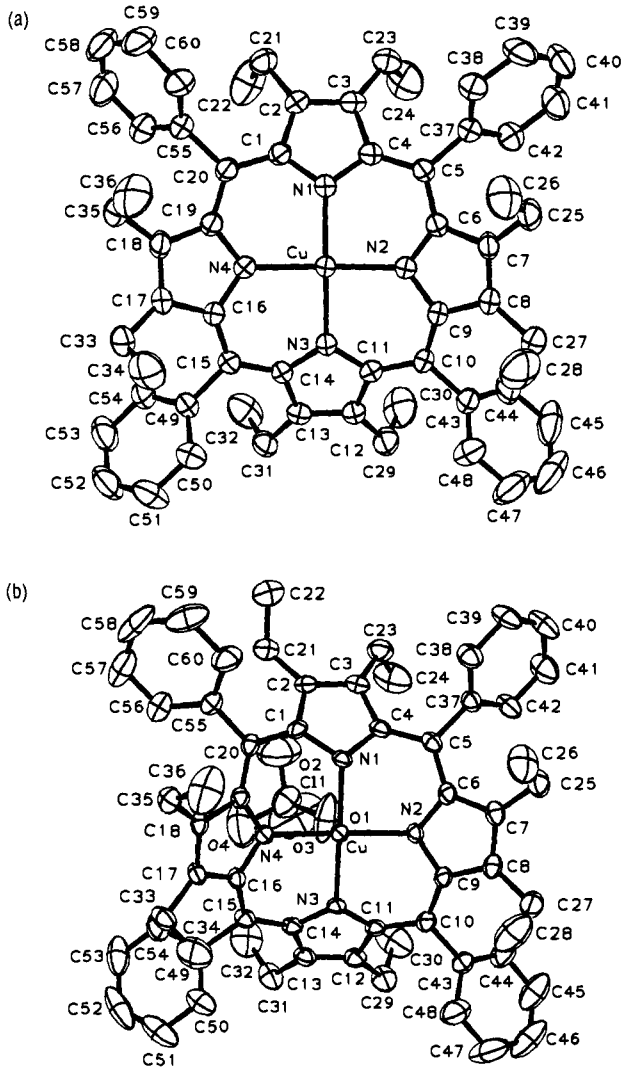

Figure 5. Molecular structures and atom numbering: (a) Cu(OETPP) and (b) $Cu(OETPP)^{\bullet+}ClO_4^-$. Thermal ellipsoids enclose 50% probability. Hydrogens are omitted for clarity.

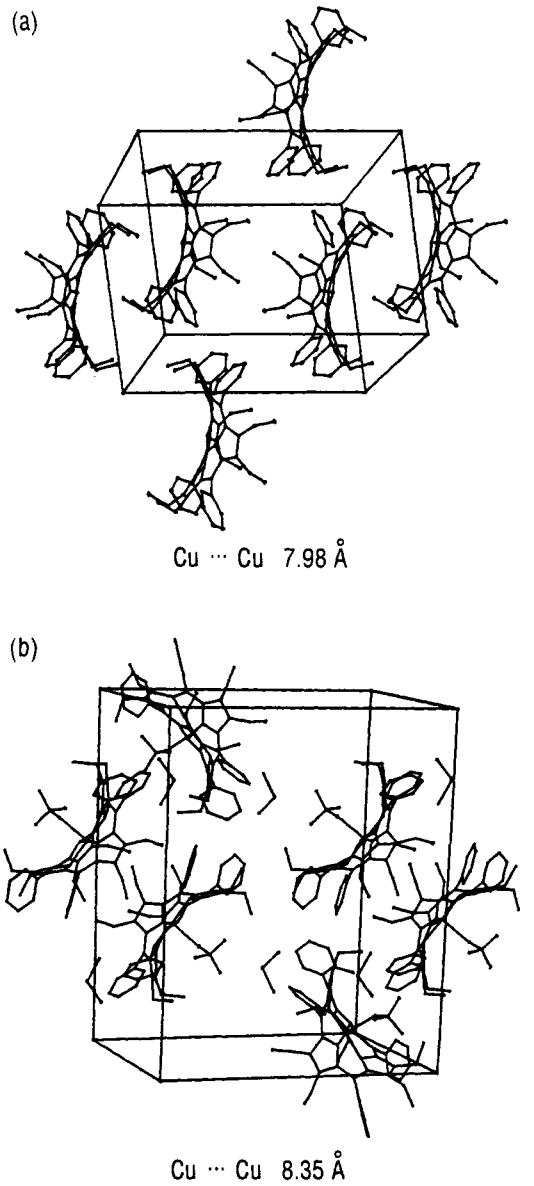

Figure 6. Packing diagrams: (a) Cu(OETPP) and (b) $Cu(OETPP)^{\bullet+}ClO_4^-$. Also shown for the latter are the carbon and two chlorine atoms of the CH_2Cl_2 of crystallization.

nitrogens are planar to ±0.04 Å but the Cu has moved out-of-plane by 0.092(1) Å toward the axial ClO_4^- counterion. The Cu–O distance to O1 of the ClO_4^- is 2.445(4) Å, a value typical of Cu–$OClO_3$ linkages, which average 2.5(1) Å in a variety of complexes.[52]

Although average N–C and C–C distances in porphyrins and porphyrin π cation radicals tend to be similar,[7,21-23] as in **1** and **2** (Table 3), specific classes of bonds change upon oxidation. For example, the Cα–Cm distances in **1** fall within the narrow range 1.400(7)–1.408(7) Å and average 1.403(7) Å. In contrast, although the same distances in **2** average 1.407 Å, they extend from 1.387(6) to 1.429(6) Å (Figure 9). The N–Cα bonds in **2** also show a larger spread, 1.361(6)–1.402(6) Å, than the corresponding bonds in **1**, 1.370(7)–1.390(7) Å. The result in **2** is a pattern of alternating shorter and longer bonds within the inner π network comprised of the nitrogen, Cα, and Cm atoms (Figure 9b). A similar pattern is present in $Cu(TPP)^{\bullet+}$ [23] and is most evident in the dimeric $ZnOEP^{\bullet+}$, as first noted by Song et al.[53] $Zn(OEP)^{\bullet+}$ is quite planar, unlike $Cu(TPP)^{\bullet+}$ or **2**, so that the effect is not simply due to the significant nonplanarity of the two Cu radicals. A_{2u} radicals do localize unpaired spin density at the nitrogens and *meso* carbons, and the 16 atom inner network might therefore be affected. The trend is not universal in all a_{2u} radicals,[21] however, or it is masked by the precision of the determinations. A_{1u} radicals with high spin density at the α carbons might be expected to show similar effects. $Zn(OEP)^{\bullet+}$ is indeed an a_{1u} radical in solution,[24] but the crystalline data are complicated by intermolecular coupling of the spins.[53] A clearer explanation for the bond alternations may evolve as additional high-precision determinations of π radicals become available. In the $Cu(TPP)^{\bullet+}$ and $Cu(OETPP)^{\bullet+}$ cases, the effect may represent a combination of a_{2u} character, antiferromagnetic coupling with the Cu(II) spin density localized at the nitrogens, and the saddle distortions. The alternation pattern is not observed (or is less obvious) in the planar, ferromagnetically coupled $Cu(TMP)^{\bullet+}$.[23]

Unlike the subtle variations in bond distances that reflect the oxidation of **1**, the conformational changes that accompany the oxidation are more obvious. **1** is severely S4 distorted, as are the H_2, H_4^{2+}, Co, Ni, and Zn members of the OETPP series.[9] The displacements of the atoms of **1** from the plane of the nitrogens and that of the 24 atoms which comprise the macrocycle are shown in Figure 7a. The pyrrole rings are tipped alternately above and below the average planes with the β carbon displacements from the nitrogen plane ranging from 1.09 to 1.21 Å while

(52) Orpen, A. G.; Brammer, L.; Allen, F. H.; Kennard, O.; Watson, D. G.; Taylor, R. *J. Chem. Soc., Dalton Trans.* **1989**, S1.

(53) Song, H.; Reed, C. A.; Scheidt, W. R. *J. Am. Chem. Soc.* **1989**, *111*, 6867.

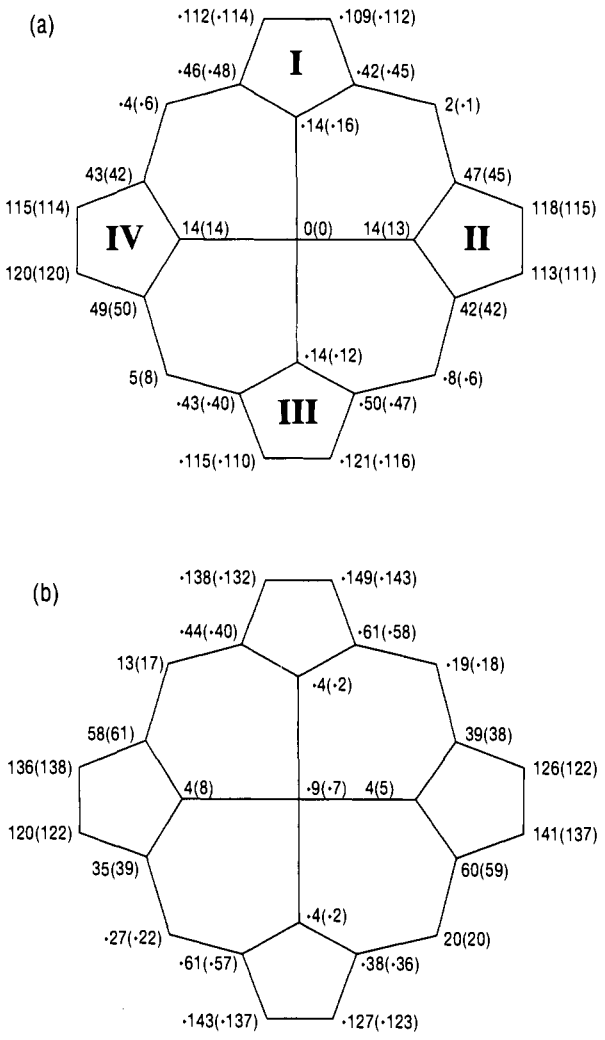

Figure 7. Displacements of the 24 atoms that comprise the porphyrin cores from the planes defined by the four nitrogens and, in parentheses, from the mean porphyrin planes, in units of 0.01 Å: (a) Cu(OETPP) and (b) $Cu(OETPP)^{\bullet+}ClO_4^-$.

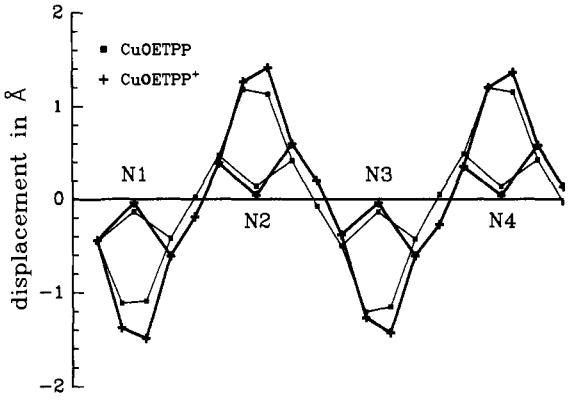

Figure 8. Linear displays of the deviations from the planes defined by the four nitrogens in Cu(OETPP) and $Cu(OETPP)^{\bullet+}ClO_4^-$ for the 24 atoms that comprise the macrocycles. (The horizontal axis is not to scale.)

the *meso* carbons lie nearly in the plane with a maximum displacement of 0.08 Å. These parameters are typical of a saddle conformation.[7,27] In contrast, in **2**, the displacements of the *meso* carbons above and below the average planes are more pronounced and deviate by as much as 0.27 Å from the nitrogen plane. As well, the pyrrole rings have rotated along the axes that bisect the nitrogens and the geminal β carbons so that the dihedral angles of the pyrrole planes relative to those of the nitrogens have increased. These angles are 40.0(2), 36.5(2), 37.4(2), and 35.2-

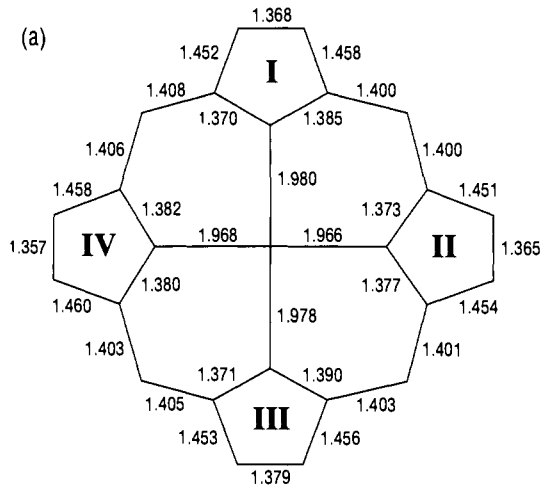

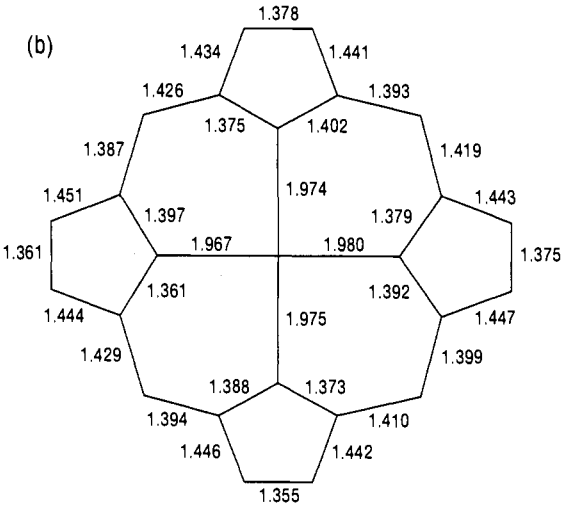

Figure 9. Comparison of the bond distances in (a) Cu(OETPP) and (b) $Cu(OETPP)^{\bullet+}ClO_4^-$. The esds are 0.007 Å for a typical C–C bond and 0.004 Å for the Cu–N distances in the neutral compound and 0.006 and 0.003 Å, respectively, in the cation.

(2)° for rings I, II, III, and IV, respectively, in the radical as opposed to 26.7(2), 28.4(2), 29.0(2), and 28.8(2)° for the same rings in **1**. The resulting increased displacements of the *meso*, α, and β carbons in **2** versus **1** are compared numerically in Figure 7 and graphically in Figure 8. The overall conformation of **2** is thus that of a saddle with some superimposed ruffling.[7,27] (Additional comparisons of average bond distances and angles in the two structures are presented in Table 3.)

A characteristic feature of all OETPP structures[9] (and of saddle conformations in *meso*-tetraarylporphyrins in general[7,27]) is the rotation of the phenyl rings into the porphyrin plane, to minimize unfavorable contacts between neighboring phenyl and ethyl groups. In **1**, the dihedral angles of the phenyl rings with the porphyrin plane range from 44.3(2) to 47.6(2)° and average 45.6°. In **2**, the dihedral angles are significantly more acute, 31.0(2), 35.1(2), 37.6(2), and 28.2(2)° for the phenyl rings at C5, 10, 15, and 20, respectively, and they average 33°. For comparison, those in $Cu(TPP)^{\bullet+}$ [23] average 41.5(10)°. (Note that, although $Cu(TPP)^{\bullet+}$ is also saddle-shaped, it is less distorted than **2**. The β carbon displacements from the mean porphyrin plane are approximately one-half (±0.6 Å) those in **2**.) In the planar $Cu(TMP)^{\bullet+}$, the phenyl dihedral angles average 82°.[23] Only in the very distorted diacid salts of tetraarylporphyrins[9e,51,54] (i.e., H_4P^{+2})

(54) Stone, A.; Fleischer, E. B. *J. Am. Chem. Soc.* **1968**, *90*, 2735. Navaza, A.; DeRango, C.; Charpin, P. *Acta Crystallogr.* **1983**, *C39*, 1625.

Table 3. Comparisons of Average Distances (Å) and Angles (deg)[a,b]

	$CuBr_8(TPFP)$,[12] 294 K	Cu(OETPP), 298 K	$Cu(OETPP)^{\bullet+}ClO_4^-$, 298 K	$Cu(TPP)^{\bullet+}SbCl_6^-$,[23] 298 K
Cu–N	1.971(6)	1.973(4)	1.974(3)	1.988(4)
N–Cα	1.380(3)	1.379(6)	1.383(6)	1.388(16)
Cα–Cβ	1.439(5)	1.455(7)	1.444(6)	1.417(17)
Cβ–Cβ	1.333(11)	1.367(7)	1.367(7)	1.336(19)
Cα–Cm	1.396(3)	1.403(7)	1.407(6)	1.400(24)
Cm–CPh	1.497(5)	1.493(7)	1.490(7)	1.487(6)
Cu–Cu	7.32	7.98	8.35	5.40
MPS	5.37	6.47	6.98	3.84
o-Ph–Cβ	3.40	3.39	3.35	3.08
o-Ph–CH_2		3.34	3.34	
Ct–N	1.969(6)	1.973(4)	1.972(4)	1.988(4)
Ct–Cα	2.976(5)	2.979(4)	2.938(3)	3.020(7)
Ct–Cm	3.373(12)	3.379(4)	3.359(2)	3.423(4)
Ph dihedral angle	46(2)	45.6(7)	33(2)	41.5(10)
N–Cu–N (adj)	90.4(3)	90.3(2)	89.9(2)	90.0(3)
N–Cu–N (opp)	171.3(2)	172.0(2)	177.1(2); 172.1(2)	177.9(4)
Cα–Cβ–Cβ	108.1(4)	106.8(4)	106.7(4)	107.6(15)
Cu–N–Cα	124.2(3)	124.5(3)	119.8(4); 122.5(3)	126.0(9)
N–Cα–Cβ	107.8(3)	109.5(4)	110.5(4)	110.1(4)
Cα–Cm–Cα	123.1(3)	123.2(4)	121.1(3)	123.1(6)
N–Cα–Cm	122.1(3)	121.8(4)	119.8(4)	123.9(12)
Cβ–Cα–Cm	129.6(2)	128.4(5)	129.5(4)	125.9(15)
Cα–N–Cα	107.6(4)	106.7(4)	105.3(4)	104.4(12)

[a] For Cu(OETPP) and $Cu(OETPP)^{\bullet+}ClO_4^-$, the number in parentheses following each averaged distance or angle is the esd of the mean or the esd for an individual measurement, whichever is larger. For $CuBr_8(TPFP)$ and $Cu(TPP)^{\bullet+}SbCl_6^-$, data are taken from refs 12 and 23 or are calculated from coordinates therein. [b] Complete sets of individual bond angles for **1** and **2** are included in the supplementary material.

do the phenyl groups exhibit the small dihedral angles observed in **2**. In spite of these acute angles in **2**, the bonds between the *meso* and phenyl carbons provide no indication of increased conjugation of the phenyl rings with the porphyrin π system. These distances average 1.493(7) Å in **1** and 1.490(7) Å in **2**.

As noted by Scheidt and Lee,[7] the distortions of the macrocycle and the phenyl dihedral angles are correlated and serve to minimize unfavorable contacts between the *ortho* phenyl carbons and hydrogens and the β pyrrole carbons and their substituents. Indeed, in spite of the different conformations of **1** and **2**, the distances between the *o*-phenyl and β carbons converge to similar values, 3.39 Å in **1**, 3.35 Å in **2**, and are ~0.2 Å longer than the equivalent values in the less distorted $Cu(TPP)^{\bullet+}$.

The molecules of **1** and **2** crystallize around centers of symmetry, as shown in Figure 6. However, in neither compound are there close intermolecular close contacts that would account for the observed conformations. In **1**, the Cu–Cu distance is 7.98 Å and the mean plane separation (MPS) between inversion-related molecules is 6.47 Å. In **2**, the Cu atoms are even further apart at 8.35 Å and the macrocycles are separated by 6.98 Å. In spite of the very distorted conformation of **2**, the separations between its molecules do not differ significantly from those of planar $Cu(TMP)^{\bullet+}$,[53] in which the Cu–Cu distance is 9.30 Å and the closest intermolecular approach is >6.7 Å. The corresponding values Cu–Cu and MPS in the saddle-shaped $Cu(TPP)^{\bullet+}$ are 5.40 and 3.84 Å, respectively. Scheidt and co-workers[7,23] attributed, quite reasonably, the nonplanarity of $Cu(TPP)^{\bullet+}$ (and of the Fe(III), Zn, and Mg(TPP) radicals[21]) to the steric constraints imposed by the dimeric close packing of the molecules in the crystals. This is clearly not the case for **2**, and its distorted conformation must therefore be attributed to the *intramolecular* steric interactions already evident in **1** plus additional electronic effects due to the radical formation. There are no obvious steric interactions with the ClO_4^- that might explain the additional distortions in **2** relative to **1**. Furthermore, the additional ruffling in **2** is not observed in $Zn(TPP)^{\bullet+}ClO_4^-$ or $Mg(TPP)^{\bullet+}ClO_4^-$,[21] in which the Ct–O distances are comparable to those in **2**.

There is one structural effect in **2** that may be attributable to the perchlorate ion. In **1**, as in all other neutral OETPPs,[9] the geminal ethyl substituents are arranged symmetrically up or down on each pyrrole ring. In **2**, the same pattern is followed except for the terminal methyl group C22 on ring I which is turned around and faces up (see Figure 5). A computer simulation suggests that, if C22 were oriented in the "expected" position, its protons would come as close as 2.3 Å to O2, one of the oxygens of the ClO_4^- that points toward ring I. It is likely therefore that the orientation of C22 is inverted in order to avoid close contact with the perchlorate ion. (An overhead view of **2** that illustrates the orientations of the ethyl groups and of the perchlorate oxygens is included in the supplementary material as Figure 3S.)

Although the crystal lattice of **2** incorporates a CH_2Cl_2 molecule of solvation, there are no close contacts between the solvate and the porphyrin (see Figure 6b). The closest approach between the CH_2Cl_2 and any portion of **2** is between its carbon, C61, and two oxygens of the ClO_4^-, O3 and O2 at 3.15 and 3.19 Å, respectively.

The question arises as to why **2** adopts a more distorted conformation than **1** since the effect is not readily ascribable to close intermolecular contacts between adjacent porphyrins or, conceivably, the CH_2Cl_2 solvate. We have already noted that the skeletal conformation of **1** is not influenced by the presence of two CH_2Cl_2 solvate molecules in the structure of **1** reported by Sparks et al.[9b] We have also pointed out that the perchlorate ion does not impose any additional ruffling on the saddles of $Zn(TPP)^{\bullet+}ClO_4$ and $Mg(TPP)^{\bullet+}ClO_4^-$, in which the Ct–O distances are similar to those in **2**. Furthermore, we have also examined crystals of **2** at 120 K. Although the refinements yielded somewhat higher *R* factors and esds ~50% greater than those at room temperature, the only distinctive feature at 120 K was a shortening of the Cu–O distance by 0.05 Å. In spite of the "closer" approach of the perchlorate to the porphyrin, the displacements of the porphyrin atoms at the two temperatures are identical within the precision of the refinements.

A more plausible explanation for the conformation of **2** comes from recent molecular mechanics calculations for nonplanar porphyrins.[55] Although there are large energy barriers to flattening or inverting nonplanar porphyrins with multiple substituents (10–20 kcal/mol),[9a,b,55] conformers with *different* degrees of nonplanarity are predicted with very small energy barriers between them. The most trivial reason for the structural differences between **1** and **2** could then simply be that we have crystallized another conformer of **1**. As well, one might argue

(55) Hobbs, J. D.; Majumder, S. A.; Luo, L.; Sickelsmith, G. A.; Quirke, J. M. E.; Medforth, C. J.; Smith, K. M.; Shelnutt, J. A. *J. Am. Chem. Soc.* **1994**, *116*, 3261.

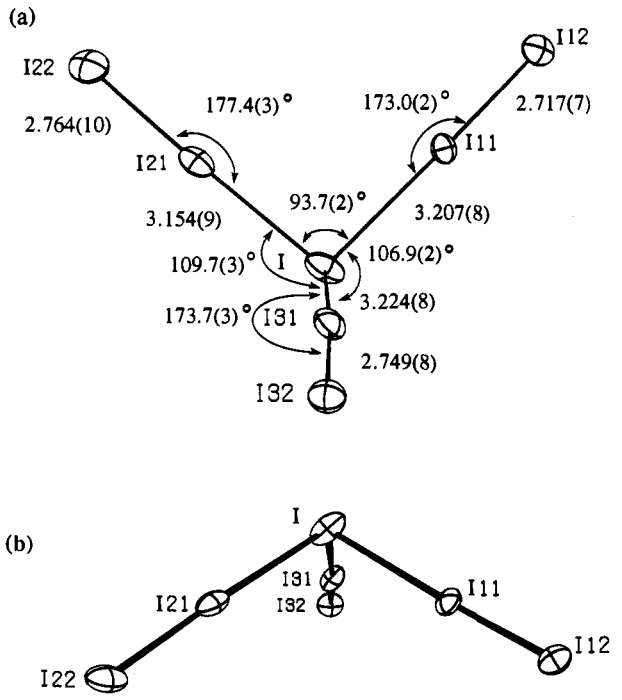

Figure 10. (a) Bond distances and angles for the I_7^- anion in Cu(OETPP)$^{\bullet+}I_7^-$. The numbers in parentheses are the esds for the last significant figure. (b) An edge-on view of the anion that illustrates its trigonal pyramid configuration.

that the rotation of the terminal methyl group on ring I is sufficient to propagate structural changes throughout the entire macrocycle. If correct, this argument implies that nonplanar porphyrins are remarkably sensitive to even small changes in their immediate environment. A more reasonable explanation is that the significant changes in electronic configuration induced by oxidation to the π cation are sufficient to overcome the small energy barriers between different conformers of already distorted molecules.[56]

Returning to the question we raised in the Introduction as to whether oxidation of nonplanar porphyrins causes conformational changes, the crystallographic results presented above certainly prove that such variations *can* occur.

We have noted above that the saddle conformation of **1** causes the molecule to be so easily oxidized that molecular iodine can oxidize it and that crystals isolated from a solution of **1** containing excess I_2 incorporate an I_7^- ion. Although polyiodide anions are well-known,[28] relatively few structures of I_7^- have been reported. Two of these consist[57] of two-dimensional networks of symmetrical I_3^- coupled to I_2 units, i.e. $[(I_3^-)\cdot 2I_2]_n$. Only recently has the first structure of a discrete I_7^-, in $P(C_6H_5)_4^+I_7^-$ (**4**), been described by Poli et al.[29] The anion in **4** assumes a trigonal pyramid configuration ascribed to an asymmetric I_3^- fragment (I–I21–I22, where I is the apical atom) interacting with two I_2 molecules (I11–I12 and I31–I32).

Polyiodides are typically associated with large cations,[28] and Cu(OETPP)$^{\bullet+}$ certainly fulfills that requirement (see also ref 30). The configuration of I_7^- in **3** is shown in Figure 10 as are bond distances and angles. The pyramidal arrangement is similar to that in **4**, and the nomenclature used by Poli et al. has been retained.

The stereochemical parameters for the two structures are compared in Table 4. The bond angles at atoms I11, I21, and I31 in **3** are all close to 180°, as in **4**, but the angles at the apical I differ by as much as 10°. The distinction between the three outer I–I distances is also less obvious in **3**, where the values are 2.72, 2.75, and 2.76 Å compared to 2.74, 2.73, and 2.81 Å in **4**. None of the outer I–I distances in **3** deviate significantly from the crystalline I_2 value of 2.72 Å.[28] The inner I–I distances in **3** are also clustered more closely together, 3.15, 3.22, and 3.21 Å vs 3.05, 3.28, and 3.30 Å in **4**. Nonetheless, if I–I11–I12 is taken as the I_3^- component of I_7^-, the two sets of bond distances in that fragment, 3.15 and 2.76 Å in **3** and 3.05 and 2.81 Å in **4**, are quite similar, respectively, to those of the asymmetric I_3^- in NH_4I_3, 3.11 and 2.79 Å,[58] and in CsI_3, 3.04 and 2.84 Å.[59] (In the polymeric I_7^- networks, the I_3^- units are symmetric with equal inner and outer distances falling between 2.90 and 2.93 Å.[57])

Table 4. Bond Distances (Å) and Angles (deg) in I_7^-

	$P(C_6H_5)_4^+I_7^-$ [29]		Cu(OETPP)$^{\bullet+}I_7^-$	
I–I21	3.051(1)	[3.05(0)][a]	3.154(9)	[3.15(1)]
I21–I22	2.814(1)	[2.81(0)]	2.764(10)	[2.76(1)]
I–I31	3.281(1)	[3.28(0)]	3.224(8)	[3.22(1)]
I31–I32	2.730(1)	[2.73(0)]	2.749(8)	[2.75(1)]
I–I11	3.295(1)	[3.30(0)]	3.207(8)	[3.21(1)]
I11–I12	2.738(1)	[2.74(0)]	2.717(7)	[2.72(1)]
interionic I–I	3.605(1)	[3.61(0)]		[3.70(1)]
I–I12–I22	173.30(4)		177.4(3)	
I–I31–I32	176.77(4)		173.7(3)	
I–I11–I12	174.38(4)		173.0(2)	
I21–I–I31	89.11(4)		109.7(3)	
I31–I–I11	85.62(3)		106.9(2)	
I21–I–I11	97.29(3)		93.7(2)	

[a] To simplify the discussion in the text, the bond distances in brackets are the rounded off values.

The packing of the ions in **3** is illustrated in the stereoview in Figure 11. The anions and cations are arranged in layers. The I_7^- units are discrete; the closest interionic distances are 3.70 Å between I32 and I12 of adjacent molecules. (In **4**, the closest interionic I–I contact is 3.61 Å.) The shortest Cu–I distance of 3.27 Å (to I12) is 0.6 Å longer than "normal" Cu–I bonds.[52] The porphyrin and iodide ions thus exist as ion pairs rather than specific complexes. As in **1** and **2**, the overall conformation of the porphyrin is also that of a saddle, not surprisingly. As in **2**, one terminal methyl group, C24, is rotated away from its expected orientation, presumably to minimize contact with I31 of a neighboring I_7^- (see Figure 11).

Concluding Remarks

We have addressed here two questions. One was a test of the proposal by Reed, Scheidt, et al.,[22,23] that nonplanar porphyrin π radicals comprised of paramagnetic metals exhibit antiferromagnetic coupling of the metal and porphyrin spins. Cu(OETPP) seemed ideally suited to test this premise since its multiple substituents induce a significant saddling of the macrocycle that would be retained in solution and would also prevent the dimerization that has complicated previous investigations. Indeed, the structure of the oxidized **2** establishes that there are no close porphyrin–porphyrin contacts. In solution, the oxidized species exhibits the optical and IR spectroscopic signatures of a π cation radical, its NMR spectrum is consistent with that of a nonplanar porphyrin, and it is clearly diamagnetic. The results are thus consonant with the proposition that the conformations of the radicals control magnetic coupling with the metals, particularly in Cu(II) π cation radicals in which the metal $d_{x^2-y^2}$ orbital is directed into the plane of the porphyrin.

We have also raised the possibility that the nonplanar BChls that comprise the primary donor in bacterial reaction centers might change their conformations upon oxidation and thereby

(56) Extrapolation of this premise to the planar Cu(TMP)$^{\bullet+}$ would then suggest that there exists a larger barrier to the rotation of the mesityl rings into the macrocycle plane required for a saddle conformation. Recall that in this radical, the mesityl rings are almost perpendicular to the porphyrin plane ($\theta > 80°$).

(57) Havinga, E. E.; Wiebenga, E. H. *Acta Crystallogr.* **1958**, *11*, 733. Hassel, O.; Hope, H. *Acta Chem. Scand.* **1961**, *15*, 407.

(58) Cheesman, G. H.; Finney, A. J. T. *Acta Crystallogr.* **1970**, *B26*, 904.

(59) Runsink, J.; Swen-Walstra, S.; Migchelsen, T. *Acta Crystallogr.* **1972**, *B28*, 1331.

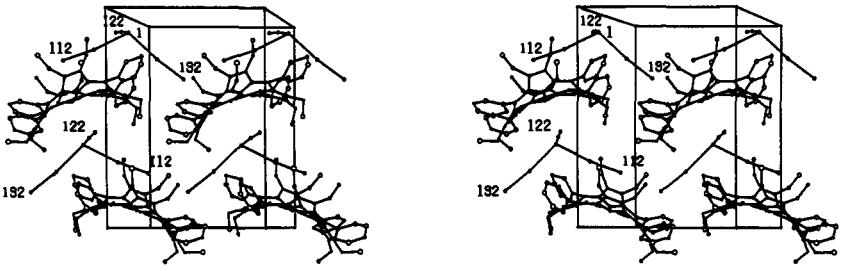

Figure 11. Stereoview of the packing of $Cu(OETPP)^{\bullet+}I_7^-$.

affect their electronic coupling with the primary electron acceptor. The crystallographic results for **2** do show nontrivial skeletal and substituent rearrangements and establish therefore that conformational changes *can* accompany oxidations. If the multiple substituents of OETPPs are taken as a primitive model of the steric constraints imposed by the protein environment of the chromophores in the reaction center, and given the high probability that oxidation of the BChls will induce some adjustments of the protein residues to the positive charge and unpaired spin density generated by the formation of a π cation,[18] it is likely that the conformation of the primary donor will be altered. (Recall that conformational substates of porphyrin–protein complexes have long been invoked in the photolysis of CO and NO heme proteins.[60]) Because the donor and acceptor lie in van der Waals contact in the reaction center, even small conformational variations would be sufficient to affect the electronic coupling between them. Indeed, large reorganizations would not favor the picosecond electron transfer in the primary charge separation.[17] The question also arises whether any structural change can occur on such a rapid time scale. In support, we note that, in the photochemistry of the rhodopsin and bacteriorhodopsin pigments, cis–trans and trans–cis isomerizations, respectively, are completed within 5 ps and the torsional transients in the isomerizations are generated within 100–300 fs.[61]

Finally, as additional evidence of the flexibility of nonplanar porphyrins, we point to recent time-resolved studies of the triplet[9d] and lowest excited singlet[15] states of H_2(OETPP) (and related molecules) which also suggest conformational excursions of the macrocycle from its ground state structure. Particularly relevant to this discussion is the large Stokes shift (850 cm^{-1}) of the H_2-(OETPP) fluorescence which clearly implies a structural reorganization in the excited singlet state.[15] Porphyrin triplets and excited singlets may be viewed simplistically as π cations and anions with unpaired and paired spins, respectively. The additional distortions observed here on oxidation of **1** to **2** may thus also contribute to the structural changes in the excited states.

Acknowledgment. This work was supported by the Division of Chemical Sciences, U.S. Department of Energy, under Contract DE-AC02-76CH00016 at Brookhaven National Laboratory, and by National Science Foundation Grant CHE-93-05577 at the University of California. C.J.M. acknowledges an Associated Western Universities/Department of Energy Postdoctoral Fellowship.

Supplementary Material Available: Tables of positional and thermal parameters for the non-hydrogen atoms of **1** and **2** at 298 K and of **3** at 200 K and bond angles for **1** and **2**, optical spectra of **2** in CH_2Cl_2 (Figure 1S), FT-IR spectra of $Cu(OETPP)^{\bullet+}PF_6^-$ in THF (Figure 2S), and an overhead view of **2** (Figure 3S) (17 pages). This material is contained in many libraries on microfiche, immediately follows this article in the microfilm version of the journal, and can be ordered from the ACS; see any current masthead page for ordering information.

(60) Ansari, A.; Berendzen, J.; Bowne, S. F.; Frauenfelder, H.; Iben, I. E. T.; Sauke, T. B.; Shyamsunder, E.; Young, R. D. *Proc. Natl. Acad. Sci. U.S.A.* **1985**, *82*, 5000. Frauenfelder, H.; Parak, F.; Young, R. D. *Annu. Rev. Biophys. Chem.* **1988**, *17*, 451.

(61) Yan, M.; Manor, D.; Weng, G.; Chao, H.; Rothberg, L.; Jedju, T. M.; Alfano, R. R.; Callender, R. H. *Proc. Natl. Acad. Sci. U.S.A.* **1991**, *88*, 9809. Pollard, W. T.; Cruz, C. H. B.; Shank, C. V.; Mathies, R. A. *J. Chem. Phys.* **1989**, *90*, 199. Petrich, J. W.; Breton, J.; Martin, J. L.; Antonetti, A. *Chem. Phys. Lett.* **1987**, *137*, 369. Nuss, M. C.; Zinth, W.; Kaiser, W.; Kolling, E.; Oesterhelt, D. *Chem. Phys. Lett.* 1985, *117*, 1.